HHS Public Access

Author manuscript

Arthroscopy. Author manuscript; available in PMC 2019 April 01.

Published in final edited form as:

Arthroscopy. 2018 April ; 34(4): 1094–1103. doi:10.1016/j.arthro.2017.10.042.

An In-vivo Prediction of Anisometry and Strain in Anterior Cruciate Ligament Reconstruction – A Combined Magnetic Resonance and Dual Fluoroscopic Imaging Analysis

Willem A. Kernkamp, MD[1,2], **Nathan H. Varady**[2], **Jing-Sheng Li**[2], **Tsung-Yuan Tsai, PhD**[1], **Peter. D. Asnis, MD**[2], **Ewoud R.A. van Arkel, MD, PhD**[3], **Rob G.H.H. Nelissen, MD, PhD**[4], **Thomas J. Gill, MD**[5], **Samuel K. Van de Velde, MD, MPH, PhD**[3], and **Guoan Li, PhD**[1]

[1]Orthopaedic Bioengineering Laboratory, Newton-Wellesley Hospital/Harvard Medical School, Newton, MA [2]Department of Orthopaedic Surgery, Massachusetts General Hospital/Harvard Medical School, Boston, MA [3]Focus Clinic Orthopedic Surgery, Haaglanden Medical Center, The Hague, The Netherlands [4]Orthopaedic Surgery, Leiden University Medical Center, Leiden, The Netherlands [5]Boston Sports Medicine and Research Institute, Dedham, MA

Abstract

Purpose—The purpose of this study was to evaluate the in-vivo anisometry and strain of theoretical ACL grafts in the healthy knee using various socket locations on both the femur and tibia.

Methods—Eighteen healthy knees were imaged using MRI and dual fluoroscopic imaging techniques during a step-up and sit-to-stand motion. The anisometry of the medial aspect of the

Corresponding Author: Guoan Li, Bioengineering Laboratory, Newton-Wellesly/Harvard Medical School, Newton, MA, 02462 Phone: +1 617 5300 563, Gli1@partners.org.

Authorship: -WA Kernkamp: Conception and design of the work, acquisition, analysis and interpretation of data for the work, drafting the work, revising it critically for important intellectual content, final approval of the version to be published.
-NH Varady: Conception and design of the work, analysis and interpretation of data, revising it critically for important intellectual content, final approval of the version to be published.
-JS Li: Conception and design of the work, analysis interpretation of data, revising it critically for important intellectual content, final approval of the version to be published.
-SK Van de Velde: Conception and design of the work, interpretation of data, revising it critically for important intellectual content, final approval of the version to be published.
-TY Tsai: Analysis and interpretation of data, revising it critically for important intellectual content, final approval of the version to be published.
-PD Asnis: Acquisition of data, revising it critically for important intellectual content, final approval of the version to be published.
-RGHH Nelissen: Conception and design of the work, acquisition, revising it critically for important intellectual content, final approval of the version to be published.
-ERA van Arkel: Conception and design of the work, acquisition, revising it critically for important intellectual content, final approval of the version to be published.
-TJ Gill: Acquisition of data, revising it critically for important intellectual content, final approval of the version to be published.
-G Li: Conception and design of the work, revising it critically for important intellectual content, final approval of the version to be published.

All authors agree to be accountable for all aspects of the work in ensuring that questions related to the accuracy or integrity of any part of the work are appropriately investigated and resolved.

lateral femoral condyle was mapped using 144 theoretical socket positions connected to an anteromedial, central and posterolateral attachment site on the tibia. The three-dimensional wrapping-paths of each theoretical graft were measured. Comparisons were made between the anatomic, over the top (OTT) and most-isometric (isometric) femoral socket locations, as well as between tibial insertions.

Results—The area of least anisometry was found in the proximal-distal direction just posterior to the intercondylar notch. The most isometric attachment site was found midway on the Blumensaat line with approximately 2% and 6% strain during the step-up and sit-to-stand motion, respectively. Posterior femoral attachments resulted in decreased graft lengths with increasing flexion angles, whereas anterodistal attachments yielded increased lengths with increasing flexion angles. The anisometry of the anatomic, OTT and isomteric grafts varied between tibial insertions ($p < 0.001$). The anatomic graft was significantly more anisometric than the OTT and isometric graft at deeper flexion angles ($p < 0.001$).

Conclusions—An area of least anisomtery was found in the proximal-distal direction just posterior to the intercondylar notch. ACL reconstruction at the isometric and OTT location resulted in non-anatomic graft behavior which could overconstrain the knee at deeper flexion angles. Tibial location significantly affected graft strains for the anatomic, OTT and isometric socket location.

Clinical Relevance—These data could be used in both biomechanical and clinical studies as a guideline to improve current intra-articular ACL reconstruction methods.

Key Terms

Anterior Cruciate Ligament; Isometry; In-vivo; Biomechanics; Fluoroscopy

Introduction

Socket positioning is one of the most critical steps in successful anterior cruciate ligament (ACL) reconstruction. ACL socket locations yielding less favorable graft behavior could lead to permanent graft stretch and graft failure. Data from the Swedish ACL registry[1] showed that more complete anatomic reconstruction reduces the risk for revision surgery. In addition, the importance of anatomic graft placement for the longevity of articular cartilage was recently emphasized by DeFrate, demonstrating how knees with grafts that more closely restored normal ACL function, and thus knee kinematics, experienced less focal cartilage thinning than did those that experienced abnormal knee motion[2].

Over the last decade, a transition has taken place encouraging more anatomic placement of the femoral socket. Consequently, the classical transtibial femoral drilling technique, which aims to minimize graft length changes during knee flexion, has made way for tibial-independent drilling techniques – e.g. anteromedial portal and outside-in retrograde drilling – which allow for more anatomic graft placement. These techniques are associated with greater length changes during knee flexion[3], however. Thus, it is paramount for surgeons to have a good understanding of the relationship between socket positioning and ACL graft length changes. As strains of 4-6% can result in permanent graft stretch and/or failure[4, 5],

correct fixation angle and tensioning may be especially important for successful clinical outcomes in anisometric ACL reconstruction.

Numerous ex-vivo studies have explored the isometry of the ACL[3, 6-9]. However, these cadaveric studies have yielded inconsistent results. Moreover, ex-vivo studies are unable to consider muscle forces that control the knee during dynamic in-vivo motion. Therefore, care should be taken when translating the ex-vivo biomechanical measurements to the results which would be seen in the knee during in-vivo weight-bearing motion and detailed information on the effect of various socket positions during in-vivo loading of the knee is lacking. Therefore, mapping the in-vivo anisometry of various theoretical ACL grafts may help improve socket placement during ACL reconstruction and surgeons' understanding of its effect on graft length.

The purpose of this study was to evaluate the in-vivo anisometry and strain of theoretical ACL grafts in the healthy knee using various socket locations on both the femur and tibia. The hypothesis was that grafts placed more posteriorly (on both the femur and tibia) would yield more anisometric behavior during knee flexion.

Methods

Participants

This study was approved by our institutional review board and written consent was obtained from each participant prior to taking part in this study project. All participants were tested between November 2008 and April 2010 to study the normal in-vivo knee kinematics during dynamic functional activities. In this study, eighteen healthy knees were studied (12 men, 6 women; age 35.4 ± 10.9 years (mean ± standard deviation); body height 175 ± 9cm; body weight 83.3 ± 18.0kg; BMI 27 ± 3.5kg/m^2, KT-1000 67N, 89N and 134N anterior forces translations were 1.8 ± 1.1 mm, 2.9 ± 1.3 mm, 4.4 ± 1.8 mm respectively) were analyzed to investigate the strain of various theoretical ACL grafts.

All participants meeting the inclusion and exclusion criteria were enrolled through our institutional broadcast e-mail announcements. The inclusion criteria consisted of participants 18 to 60 years old with the ability to perform daily activities independently without any assistance device and without taking pain medication. Standard knee examination was performed on the knee, including the Lachman and anterior drawer test, and participants with increased laxity were excluded. Other exclusion criteria were knee pain, previous knee injury, and previous surgery to the studied lower limb. The magnetic resonance imaging (MRI) scan of the knee of each participant was assessed for potential meniscal tears, chondral defects, and ligamentous injuries; if present, the participant was excluded from further analysis.

Imaging procedure

The MRI and dual fluoroscopic imaging techniques for the measurement of ligament kinematics have been described in detail previously[10]. MRI scans of the knee joints were done in both sagittal and coronal planes using a 3-Tesla MRI scanner (MAGNETOM Trio, Siemens, Malvern, PA) with a double-echo water-excitation sequence (thickness 1 mm;

resolution of 512 × 512 pixels)[11]. The images were then imported into solid modeling software (Rhinoceros; Robert McNeel and Associates, Seattle, WA, USA) to construct three-dimensional (3D) surface models of the tibia, fibula and femur.

The knee of each participant was simultaneously imaged using two fluoroscopes (BV Pulsera, Philips, the Netherlands) as the participant performed a step-up (55 ± 4°) and sit-to-stand motion (88 ± 10°). Next, the fluoroscopic images were imported into solid modeling software and placed in the imaging planes based on the projection geometry of the fluoroscopes during imaging of the participant. Finally, the MRI-based knee model of each participant was imported into the software, viewed from the directions corresponding to the fluoroscopic X-ray source used to acquire the images, and independently manipulated in six-degrees-of-freedom inside the software until the projections of the model matched with the outlines of the fluoroscopic images. When the projections best matched the outlines of the images taken during in-vivo knee motion, the positions of the models were considered to be reproductions of the in-vivo 3D positions of the knees. This system has an error of <0.1mm and 0.3° in measuring tibiofemoral joint translations and rotations, respectively[10-12].

Tibial attachment points

In order to determine the in-vivo length patterns of theoretical grafts during motion, various tibial and femoral attachment sites were used. The tibial attachment areas of the ACL were determined based on the MR images in both sagittal and coronal planes[13]. The anatomic ACL attachment area was directly mapped onto the 3D MRI-based tibia model. The attachment area was then subdivided into an anteromedial and posterolateral portion guided by the meticulously performed anatomic descriptions of Edwards et al[14] and Ferretti et al[15]. The geometrical centers of the ACL, anteromedial and posterolateral attachment areas were determined and used as three distinct tibial attachment points (Figure 1).

Femoral attachment points

A true medial view of the femur was established (perpendicular to the medial-lateral femoral axis). To account for the geometric variations between knees, a quadrant method (4×4 grid) developed by Bernard et al[16] was applied to the 3D-models. The most anterior edge of the femoral notch roof was chosen as the reference for the grid alignment (line *h*), i.e. the Blumensaat line (which in fact is a derivative of the true Blumensaat line, since the latter is a radiograph finding, while the line used in the current study was based on 3D-models)[17]. The segments along line *h* and perpendicular to line *h* (line *t*) were divided into fourths. The medial view was used to project 144 femoral attachment points to the medial aspect of the lateral femoral condyle (Figure 2A). The region of interest for the femoral points was determined by the bony edges of the medial aspect of the lateral femoral condyle, i.e. using the cartilage as borders. The region of interest was then further dived into 16 sub-areas (Figure 2B). Finally, the anatomic and transtibial over the top (OTT) ACL socket locations were identified based on Parkar et al[18].

Strain measurements

The length changes for each theoretical graft were measured as a function of knee flexion. The direct line connecting the femoral and tibial attachment point was projected on the bony

surfaces. This allowed to create a line that avoids penetration through bone, and therefore followed bony geometry, i.e. a wrapping path (Figure 3). An optimization procedure was implemented to determine the projection angle to find the shortest 3D wrapping path (this is to mimic a path of minimal resistance) at each flexion angle of the knee. This technique has been described in previous studies for measurements of ligament kinematics[19]. The length of the projected line (i.e. curved around the bony surfaces) was measured as the length of the graft. Following the methods by Taylor et al[20], ACL strain was measured from the ACL length changes relative to a reference as follows:

$$\varepsilon = \frac{L - L_0}{L_0} \times 100\,\%$$

Where $\boldsymbol{\varepsilon}$ is relative graft strain, $\mathbf{L}$ is graft length, and $\mathbf{L_0}$ is a reference length (defined as the length of the non-weight-bearing MR imaging position).

A heat map was created to provide visual representation of the anisometry distribution over the medial aspect of the lateral femoral condyle by using the *mean maximum strain – mean minimum strain* of each theoretical tibiofemoral graft during both motions.

Statistics

Data were first pooled according to tibial attachment sites. A two-way analysis of variance (ANOVA) was used to assess for differences in mean anisometry due to tibial attachment sites, flexion angle, and their interaction. Then, for each femoral attachment site, a two-way ANOVA was used to examine differences in anisometry between the three studied tibial attachments. If significant, Tukey's honestly significant difference (HSD) post hoc tests were performed to compare between pairs of the three individual tibial socket positions.

A similar procedure was then implemented with data pooled by femoral attachment site. A two-way analysis of variance was used to assess for differences in mean anisometry due to femoral attachment sites, flexion angle, and their interaction. Then, for each tibial attachment site, a two-way ANOVA was used to examine differences in anisometry between the three studied femoral attachments. If significant, Tukey's HSD post hoc tests were performed to compare between pairs of the three individual femoral socket positions. In contrast to the tibial pool, the interaction between femoral socket location and flexion angle was significantly associated with anisometry patterns for the femoral sockets. Therefore, Tukey's HSD tests were also employed to examine differences between the femoral socket positions at each flexion angle. All analyses were performed in R version 3.3.2 and P-values less than 0.05 were considered significant.

Results

Posterior to the femoral intercondylar notch, running in the proximal-distal direction, a zone demonstrated least anisometry during the step-up and sit-to-stand motions (i.e. the blue area on the medial aspect of the lateral femoral condyle in Figure 4A-B, Figure 5A-B). The most isometric attachment location when connected to the anteromedial, central or posterolateral

tibial attachments for each activity is described in Table 1. Attachments located posteriorly to the isometric zone resulted in decreased graft lengths with increasing flexion angles (Figure 6A-B), whereas distal-anterior grafts increased in length with increasing flexion angles. The anisometry heatmap during both the step-up and sit-to-stand motion is illustrated in video 1.

Femoral comparison

During step-up and sit-to-stand motion, when the femoral bundles were connected to any of the three tibial locations, the isometric attachment was significantly more isometric than the anatomic ($p < 0.001$) and the OTT location ($p < 0.001$); the OTT location was significantly more isometric than the anatomic ($p < 0.001$) (Table 2A, B). When connected to the central tibial location, significant differences in strain were found between the anatomic vs. isometric locations from 20-50° degrees of flexion ($p < 0.001$), anatomic vs. OTT from 25-50° of flexion (25° $p = 0.004$, 30-50° $p < 0.001$) and for the isometric vs OTT location from 30-50° of flexion (30° $p = 0.03$, 40-50° $p < 0.001$) (Figure 7A, Table 3A). Results for the sit-to-stand motion are mentioned in Figure 7B, Table 3B.

Tibial comparison

For the step-up motion, when connected to the isometric femoral socket, no significant differences in anisometry were found between the anteromedial and central ($p = 0.14$) or central and posterolateral ($p = 0.15$) tibial attachments; the anteromedial and posterolateral tibial attachment were significantly different ($p < 0.001$). When grafts were attached the anatomic femoral socket, the anteromedial and central tibial attachments were not statistically different ($p = 0.08$); significant differences were found between the anteromedial and posterolateral ($p < 0.001$), and central and posterolateral attachments ($p = 0.017$). When connected to the OTT socket location, significant differences in mean isometry were found between the anteromedial and central attachment ($p = 0.003$), and the anteromedial and posterolateral attachment ($p < 0.001$), and the central and posterolateral attachment ($p < 0.001$) (Table 2A). Results for the sit-to-stand motion are mentioned in Table 2B.

Discussion

In this study, the most isometric femoral socket location was approximately midway on the Blumensaat line just posterior to the intercondylar femoral notch. This was true for the three studied tibial attachments (i.e. anteromedial, central, and posterolateral location) during both motions. A graft in this position underwent approximately 2% and 6% strain during the step-up and sit-to-stand motion respectively. The theoretical ACL strains were most affected by changing the femoral socket positions in the anterior-posterior direction. Posterior femoral attachments resulted in decreased lengths with increasing flexion angles, whereas anterior-distal grafts increased in length with increasing flexion angles.

Traditional thinking in ACL reconstruction has focused on avoiding peak graft strains at full-extension, as strains greater than 4-6% are known lead to undesirable graft behavior — namely over-constraint and potentially graft failure[4, 5]. Therefore, depending on the tibiofemoral socket positions, and thus the anisometry pattern, the fixation angle is a crucial

variable in achieving desirable graft behavior. This is especially true for anisometric grafts which experience greater length changes over knee range-of-motion. As evidenced by this study, anteriorly positioned femoral sockets show less length change, particularly pronounced during the extension to early flexion range, than more posteriorly positioned sockets, which greatly decrease in length with increasing flexion (Figure 6). For example, graft fixation at 30° of flexion may have detrimental consequences if one prefers to place the femoral socket posteriorly (e.g. quadrants B3-4) over time because of repetitive stretch-shortening cycles from 30° to full extension. This may be especially important for the posterolateral socket during double bundle ACL reconstruction. In contrast, a surgeon may have more flexibility in fixation angle when aiming for anterior socket positioning.

Given the importance of avoiding peak strains it may be surprising that isometric ACL reconstruction techniques are not associated with improved clinical outcomes. However, our study demonstrates that the most isometric point on the femur is located far from the anatomic ACL insertion site (Figure 4, 5). This means that a socket drilled at the isometric location (i.e. distal and anterior to the center of the ACL footprint) will result in a non-anatomic ACL reconstruction. In fact, given their relatively constant strains, isometric and OTT grafts may experience a relatively higher strain at deeper flexion angles than an anatomic ACL reconstruction. Specifically, the isometric and OTT locations had significantly higher strains than the anatomic location (i.e. strains closer to their 0° strain, while the anatomic ACL decreased more in relative length) beyond approximately 20° of knee flexion. The theoretical isometric and OTT grafts yielded more isometric behavior, and are therefore relatively “longer” than an anatomic ACL reconstruction. These increased relative strains compared the anatomic reconstruction may account for the lack of improved clinical outcomes with non-anatomic reconstructions[2, 21]. Previous studies evaluating socket position in revision ACL reconstruction cases found a tendency of more anteriorly placed femoral socket and posteriorly placed tibial socket[22-24]. While these grafts might in theory have been relatively isometric based on the anterior femoral attachment, the biomechanically inadequate orientation of the graft could have placed the reconstruction at risk of failure.

Recent anatomic studies have revealed two types of femoral attachment fibers of the ACL, namely a direct type and an indirect type[25-27]. In the in-vitro setting, simulated tests of uniplanar anterior and combined anterior and rotatory loads have indicated that the direct attachment serves primarily in restraining anterior tibial translation[28-30]. In addition, Nawabi et al[30] found the direct attachment to form a key link in transmitting mechanical load to the joint (i.e. bear more force) and to be more isometric than the indirect attachment. Kawaguchi et al[29] showed that the direct attachment (areas G and H in their study) of the ACL resisted 82-90% of the anterior drawer force, with most load carried by the fibers closest to the roof of the intercondylar notch (66-84%). Interestingly, this key region for force transfer (area G and H[29]) is located near the isometric area (dark blue zone in Figure 4) during in-vivo knee flexion as demonstrated by our study. Given DeFrate's recent work[2] demonstrating the importance of restoring functional anatomy and the concordance of isometry between recent ex-vivo studies and this in-vivo study, these results may encourage future research elucidating functional anatomic ACL reconstruction techniques focused on restoring the anteriorly located direct fibers of the ACL.

Another variable that is directly related to the socket position is the functional length of the graft, which is an important variable in any ligament reconstruction. Stress-strain curves consist of a nonlinear toe region and a linear region. Long grafts undergo greater elongation under the same load compared with short grafts for both nonlinear and linear regions. This means that decreasing the length of a graft, i.e. a femoral socket that has close proximity to the tibial socket, linearly increases its stiffness[31]. Therefore, the socket position of the ACL graft determines the effective length and thus plays an important role in the kinematic response of the knee. In the current study, it was found that the tibial location significantly affected the mean anisometry. In the recent study by Inderhaug et al[32] it was shown that posterior tibial socket positioning was related to an increased rate of revision cases. Future studies may further explore the effect and its significance of the tibial socket positioning.

The present description of in-vivo graft anisometry at various positions is critical information for further follow-up studies on graft behavior and clinical outcome. Independent of surgical technique, these data could help surgeons to improve the socket position and fixation angle. Moreover, these data may be useful in the setting of ACL revision; while previous studies have typically only examined the anatomic ACL insertion site, this study provides a map of the entire medial aspect of the lateral femoral condyle, which may be useful if the anatomic site is compromised.

Limitations

There are several limitations to this study. Only data from healthy knees during two functional activities were used. No full range-of-motion activity was studied, more specifically, no hyperextension or flexion angles beyond 90° of flexion were analyzed. Future research should consider knees with a torn ACL and more demanding in-vivo functional activities (e.g. lunging, running and jumping). No pivoting motion was performed in this study and thus the effect of excessive rotational moments could not be assessed.. In this study, strain was measured using the reference length as measured from the non-weightbearing MR imaging position. The precise reference lengths (zero-load length) are unknown due to the in-vivo nature of the study. However, previously this measurement has been shown to be linearly related to the true strain[20]. Finally, no actual ACL reconstructions were performed in the present study, so no definite conclusions could be generated regarding the most optimal socket positions.

Conclusion

An area of least anisomtery was found in the proximal-distal direction just posterior to the intercondylar notch. ACL reconstruction at the isometric and OTT location resulted in non-anatomic graft behavior which could overconstrain the knee at deeper flexion angles. Tibial location significantly affected graft strains for the anatomic, OTT and isometric socket location.

Supplementary Material

Refer to Web version on PubMed Central for supplementary material.

Acknowledgments

Source of Funding National Institutes of Health (NIH) grant R-01 AR055612

References

1. Svantesson E, Sundemo D, Hamrin Senorski E, et al. Double-bundle anterior cruciate ligament reconstruction is superior to single-bundle reconstruction in terms of revision frequency: a study of 22,460 patients from the Swedish National Knee Ligament Register. Knee Surg Sports Traumatol Arthrosc. 2016
2. DeFrate LE. The effects of ACL graft placement on in vivo knee function and cartilage thickness distributions. J Orthop Res. 2017
3. Lubowitz JH. Anatomic ACL reconstruction produces greater graft length change during knee range-of-motion than transtibial technique. Knee Surg Sports Traumatol Arthrosc. 2014; 22:1190–1195. [PubMed: 24077671]
4. Zavras TD, Race A, Bull AM, Amis AA. A comparative study of 'isometric' points for anterior cruciate ligament graft attachment. Knee Surg Sports Traumatol Arthrosc. 2001; 9:28–33. [PubMed: 11269581]
5. Penner DA, Daniel DM, Wood P, Mishra D. An in vitro study of anterior cruciate ligament graft placement and isometry. Am J Sports Med. 1988; 16:238–243. [PubMed: 3381980]
6. Lee JS, Kim TH, Kang SY, et al. How isometric are the anatomic femoral tunnel and the anterior tibial tunnel for anterior cruciate ligament reconstruction? Arthroscopy. 2012; 28:1504–1512. 1512 e1501–1502. [PubMed: 22739002]
7. Wang JH, Kato Y, Ingham SJ, et al. Measurement of the end-to-end distances between the femoral and tibial insertion sites of the anterior cruciate ligament during knee flexion and with rotational torque. Arthroscopy. 2012; 28:1524–1532. [PubMed: 22717210]
8. Hefzy MS, Grood ES, Noyes FR. Factors affecting the region of most isometric femoral attachments. Part II: The anterior cruciate ligament. Am J Sports Med. 1989; 17:208–216. [PubMed: 2667378]
9. Sidles JA, Larson RV, Garbini JL, Downey DJ, Matsen FA 3rd. Ligament length relationships in the moving knee. J Orthop Res. 1988; 6:593–610. [PubMed: 3379513]
10. Li G, Van de Velde SK, Bingham JT. Validation of a non-invasive fluoroscopic imaging technique for the measurement of dynamic knee joint motion. J Biomech. 2008; 41:1616–1622. [PubMed: 18394629]
11. Defrate LE, Papannagari R, Gill TJ, Moses JM, Pathare NP, Li G. The 6 degrees of freedom kinematics of the knee after anterior cruciate ligament deficiency: an in vivo imaging analysis. Am J Sports Med. 2006; 34:1240–1246. [PubMed: 16636348]
12. Li G, Wuerz TH, DeFrate LE. Feasibility of using orthogonal fluoroscopic images to measure in vivo joint kinematics. J Biomech Eng. 2004; 126:314–318. [PubMed: 15179865]
13. Hosseini A, Gill TJ, Li G. In vivo anterior cruciate ligament elongation in response to axial tibial loads. J Orthop Sci. 2009; 14:298–306. [PubMed: 19499297]
14. Edwards A, Bull AM, Amis AA. The attachments of the anteromedial and posterolateral fibre bundles of the anterior cruciate ligament: Part 1: tibial attachment. Knee Surg Sports Traumatol Arthrosc. 2007; 15:1414–1421. [PubMed: 17934717]
15. Ferretti M, Doca D, Ingham SM, Cohen M, Fu FH. Bony and soft tissue landmarks of the ACL tibial insertion site: an anatomical study. Knee Surg Sports Traumatol Arthrosc. 2012; 20:62–68. [PubMed: 21710110]
16. Bernard M, Hertel P, Hornung H, Cierpinski T. Femoral insertion of the ACL. Radiographic quadrant method. Am J Knee Surg. 1997; 10:14–21. discussion 21-12. [PubMed: 9051173]
17. Forsythe B, Kopf S, Wong AK, et al. The location of femoral and tibial tunnels in anatomic double-bundle anterior cruciate ligament reconstruction analyzed by three-dimensional computed tomography models. J Bone Joint Surg Am. 2010; 92:1418–1426. [PubMed: 20516317]
18. Parkar AP, Adriaensen M, Vindfeld S, Solheim E. The Anatomic Centers of the Femoral and Tibial Insertions of the Anterior Cruciate Ligament: A Systematic Review of Imaging and Cadaveric

Studies Reporting Normal Center Locations. The American journal of sports medicine. 2017; 45:2180–2188. [PubMed: 27899355]

19. Van de Velde SK, DeFrate LE, Gill TJ, Moses JM, Papannagari R, Li G. The effect of anterior cruciate ligament deficiency on the in vivo elongation of the medial and lateral collateral ligaments. Am J Sports Med. 2007; 35:294–300. [PubMed: 17092925]
20. Taylor KA, Terry ME, Utturkar GM, et al. Measurement of in vivo anterior cruciate ligament strain during dynamic jump landing. Journal of biomechanics. 2011; 44:365–371. [PubMed: 21092960]
21. Jaecker V, Zapf T, Naendrup JH, et al. High non-anatomic tunnel position rates in ACL reconstruction failure using both transtibial and anteromedial tunnel drilling techniques. Archives of orthopaedic and trauma surgery. 2017
22. Hosseini A, Lodhia P, Van de Velde SK, et al. Tunnel position and graft orientation in failed anterior cruciate ligament reconstruction: a clinical and imaging analysis. Int Orthop. 2012; 36:845–852. [PubMed: 21826407]
23. Parkinson B, Robb C, Thomas M, Thompson P, Spalding T. Factors That Predict Failure in Anatomic Single-Bundle Anterior Cruciate Ligament Reconstruction. Am J Sports Med. 2017; 363546517691961
24. Trojani C, Sbihi A, Djian P, et al. Causes for failure of ACL reconstruction and influence of meniscectomies after revision. Knee Surg Sports Traumatol Arthrosc. 2011; 19:196–201. [PubMed: 20644911]
25. Mochizuki T, Fujishiro H, Nimura A, et al. Anatomic and histologic analysis of the mid-substance and fan-like extension fibres of the anterior cruciate ligament during knee motion, with special reference to the femoral attachment. Knee Surg Sports Traumatol Arthrosc. 2014; 22:336–344. [PubMed: 23344119]
26. Sasaki N, Ishibashi Y, Tsuda E, et al. The femoral insertion of the anterior cruciate ligament: discrepancy between macroscopic and histological observations. Arthroscopy. 2012; 28:1135–1146. [PubMed: 22440794]
27. Smigielski R, Zdanowicz U, Drwiega M, Ciszek B, Williams A. The anatomy of the anterior cruciate ligament and its relevance to the technique of reconstruction. The bone & joint journal. 2016; 98-b:1020–1026. [PubMed: 27482012]
28. Pathare NP, Nicholas SJ, Colbrunn R, McHugh MP. Kinematic analysis of the indirect femoral insertion of the anterior cruciate ligament: implications for anatomic femoral tunnel placement. Arthroscopy. 2014; 30:1430–1438. [PubMed: 25241294]
29. Kawaguchi Y, Kondo E, Takeda R, Akita K, Yasuda K, Amis AA. The role of fibers in the femoral attachment of the anterior cruciate ligament in resisting tibial displacement. Arthroscopy. 2015; 31:435–444. [PubMed: 25530509]
30. Nawabi DH, Tucker S, Schafer KA, et al. ACL Fibers Near the Lateral Intercondylar Ridge Are the Most Load Bearing During Stability Examinations and Isometric Through Passive Flexion. Am J Sports Med. 2016; 44:2563–2571. [PubMed: 27440804]
31. DeFrate LE, van der Ven A, Gill TJ, Li G. The effect of length on the structural properties of an Achilles tendon graft as used in posterior cruciate ligament reconstruction. Am J Sports Med. 2004; 32:993–997. [PubMed: 15150048]
32. Inderhaug E, Raknes S, Ostvold T, Solheim E, Strand T. Increased revision rate with posterior tibial tunnel placement after using the 70-degree tibial guide in ACL reconstruction. Knee surgery, sports traumatology, arthroscopy : official journal of the ESSKA. 2017; 25:152–158.

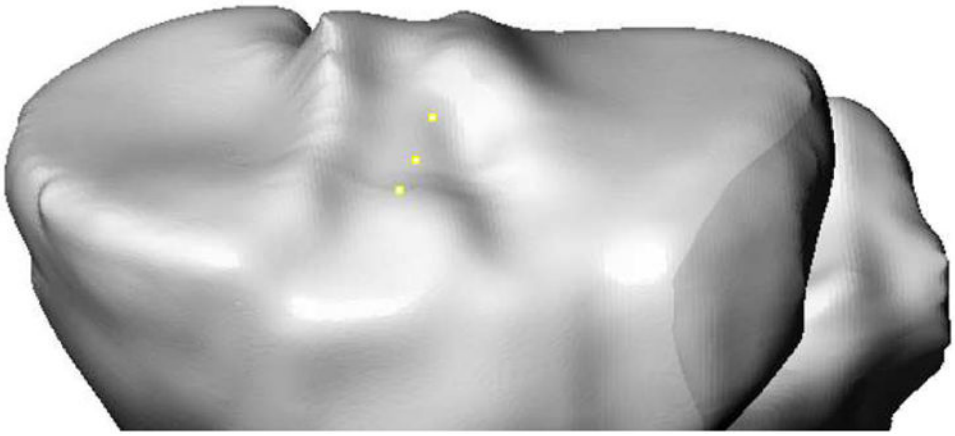

Figure 1.
Proximal-distal view of a 3D tibia and fibula model showing the distribution of the anteromedial, central and posterolateral tibial attachment points.

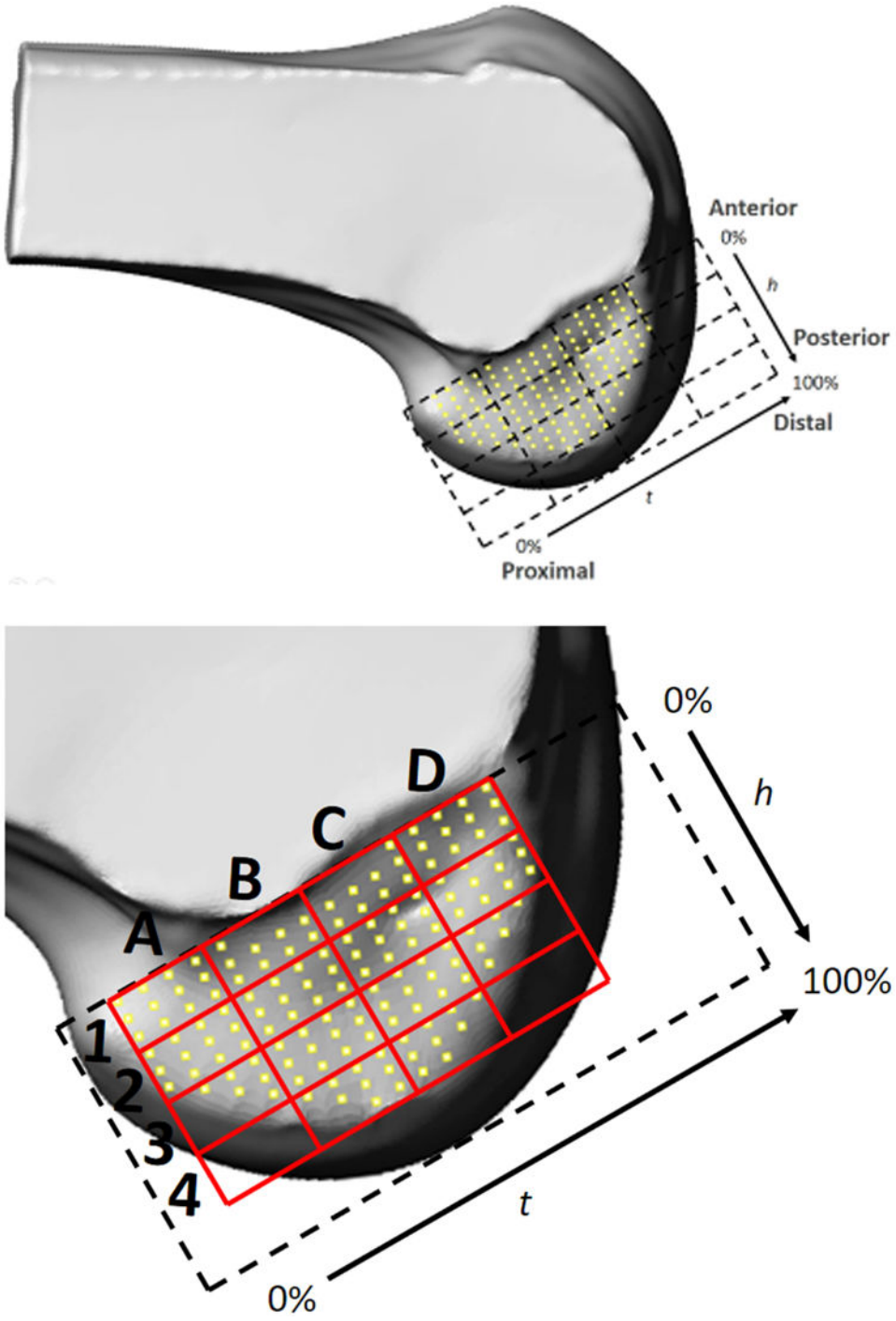

Figure 2.

(A) Medial view of a 3D femur model in 90° of flexion. The 4×4 grid as developed by Bernard et al,[16] was applied to the medial aspect of the lateral femoral condyle. A line extending along the Blumensaat line was used as a landmark for the anterior border of the grid (line *t*). Parallel to line *t* a line was drawn to the posterior edge of the lateral condyle to form the posterior border. The proximal and distal borders were formed by two lines

perpendicular to the Blumensaat line (line *h*) originating from the proximal and distal bony borders of the lateral femoral condyle. Line *h*: maximum distance from the proximal condylar bony border to femoral joint line. Line *t*: maximum distance perpendicular from the Blumensaat to the posterior edge of the lateral condyle. **(B)** The medial view was used to project 144 femoral attachment points to the medial aspect of the lateral femoral condyle. The region of interest for the femoral points was determined by the bony edges of the medial aspect of the lateral femoral condyle, i.e. using the cartilage as borders. The region of interest was then further dived into 16 sub-areas. Distal to proximal direction A to D; anterior to posterior direction 1 to 4.

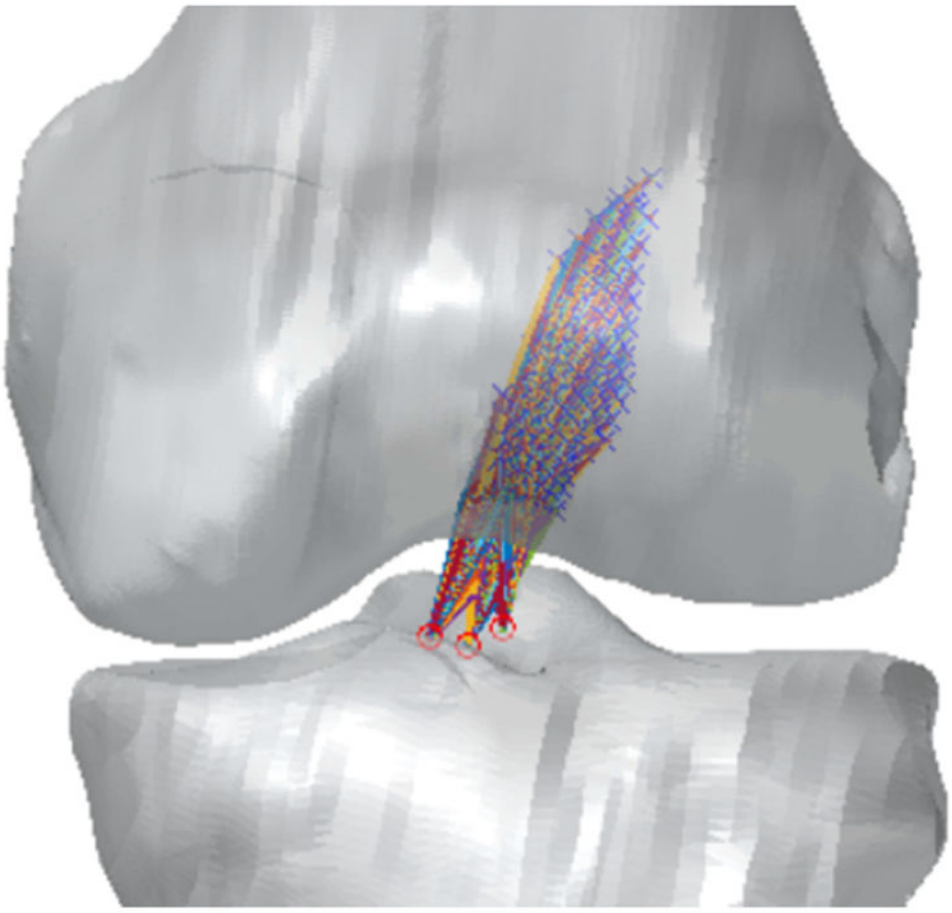

Figure 3.
Anterior-posterior view of a 3D knee model illustrating the lines curving over the bony geometry of the femur and tibia, i.e. the “wrapping effect”. At each flexion angle, an optimization procedure was implemented to determine the graft projection angle to find the shortest 3D wrapping path, mimicking the path of least resistance for the ACL graft.

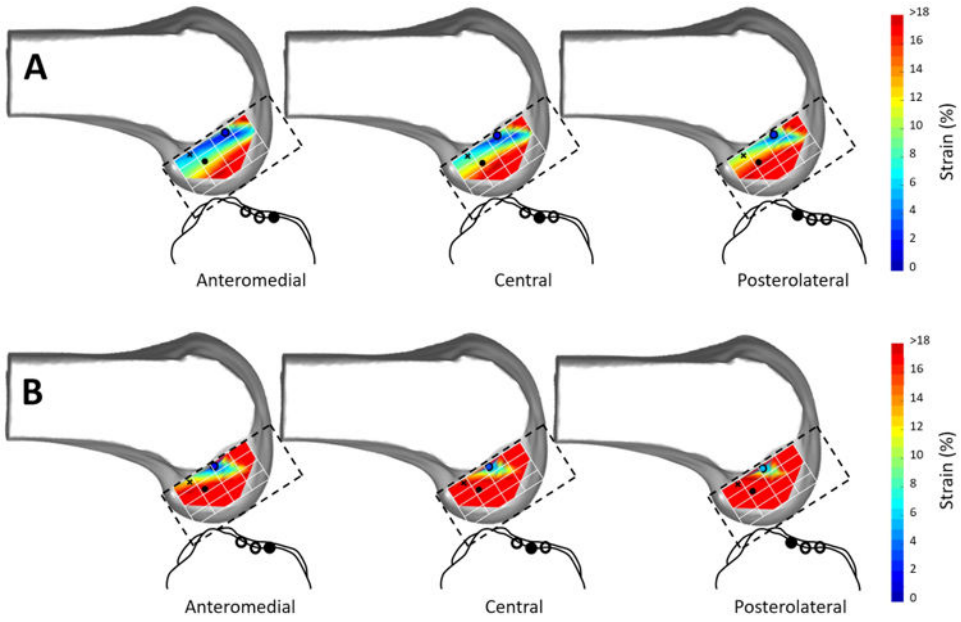

Figure 4.

Medial view of a 3D femur model in 90° of flexion. The "heat map" illustrates the isometry distribution (mean *maximum strain – minimum strain*) over the medial aspect of the lateral femoral condyle for single point-to-point curves when connected to anteromedial, central or posterolateral tibial attachment during the dynamic step-up **(A)** and sit-to-stand motion **(B)**. The darkest blue area on the femur represents the most isometric attachment area, while red areas highlights areas with a high degree of anisometry. Specifically, the circle represents the most isometric attachment. The black cross (x) on the femur shows the "over the top" position as would be achieved by transtibial drilling; the black dot shows the center of the ACL footprint as described by Parkar et al[18].

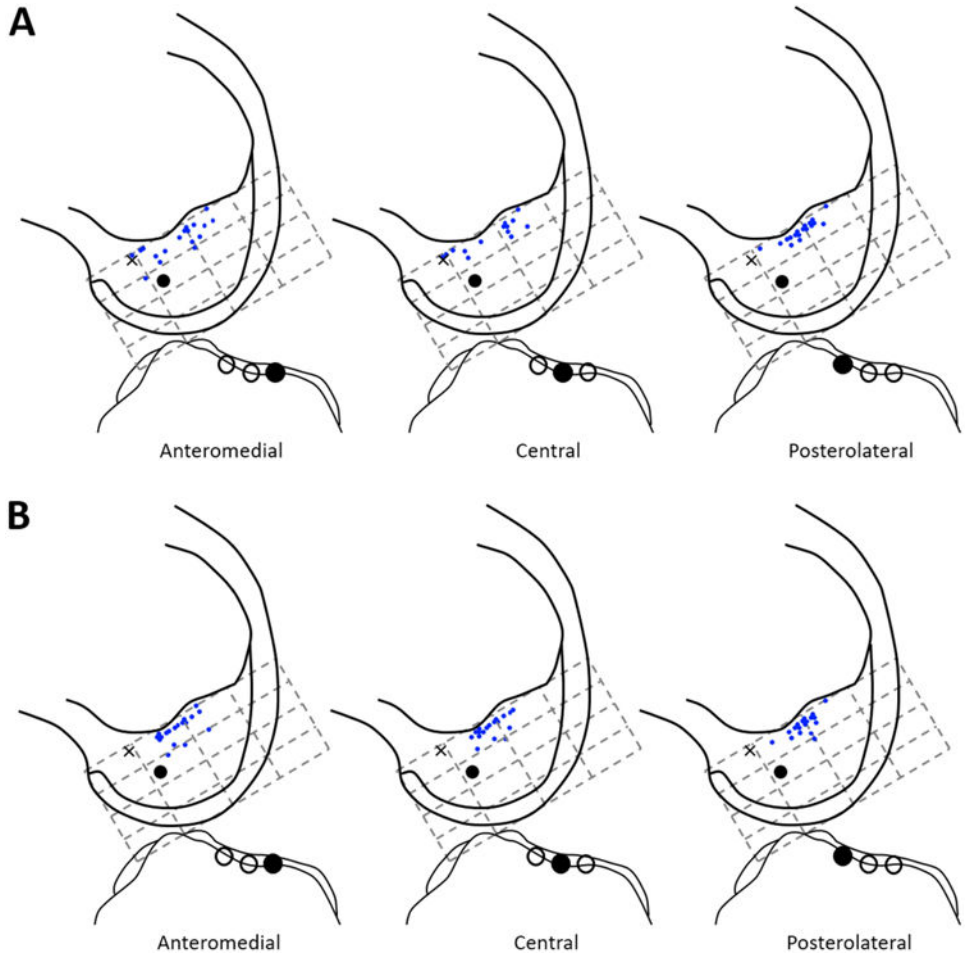

Figure 5.

Medial view of a schematic femur model in 90° of flexion. The most isometric location (mean *maximum strain – minimum strain*) on the medial aspect of the lateral femoral condyle per participant is illustrated when connected to anteromedial, central or posterolateral tibial attachment during the dynamic step-up **(A)** and sit-to-stand motion **(B)**. The black cross (x) on the femur shows the "over the top" position as would be achieved by transtibial drilling; the black dot shows the center of the ACL footprint as described by Parkar et al[18].

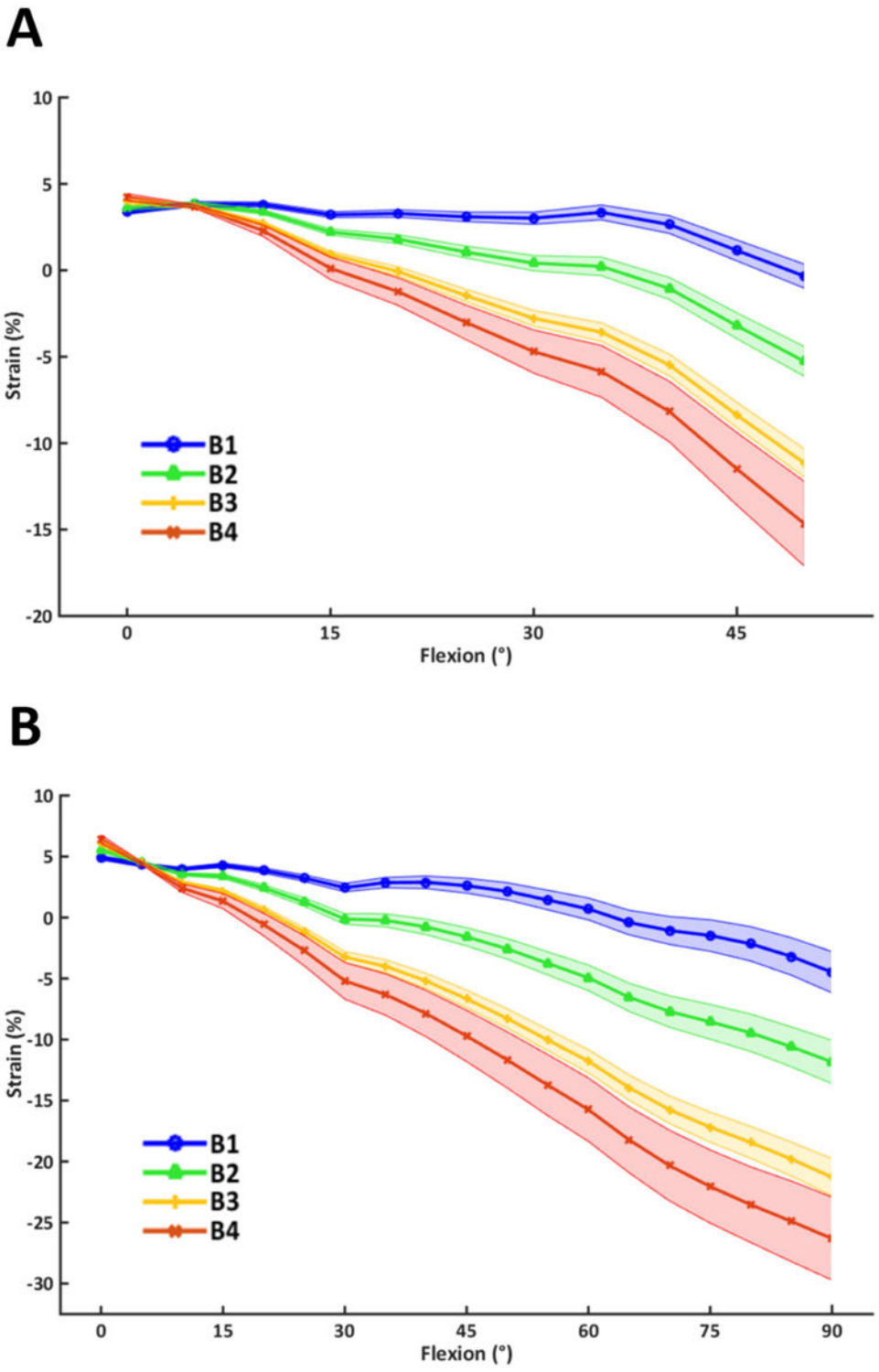

Figure 6.

Strain per area in the anterior to posterior direction e.g. B1 (anterior) to B4 (posterior) during the dynamic step-up **(A)** and sit-to-stand **(B)** motion when connected to the anteromedial tibial attachment. Values are presented as mean and 95% confidence interval.

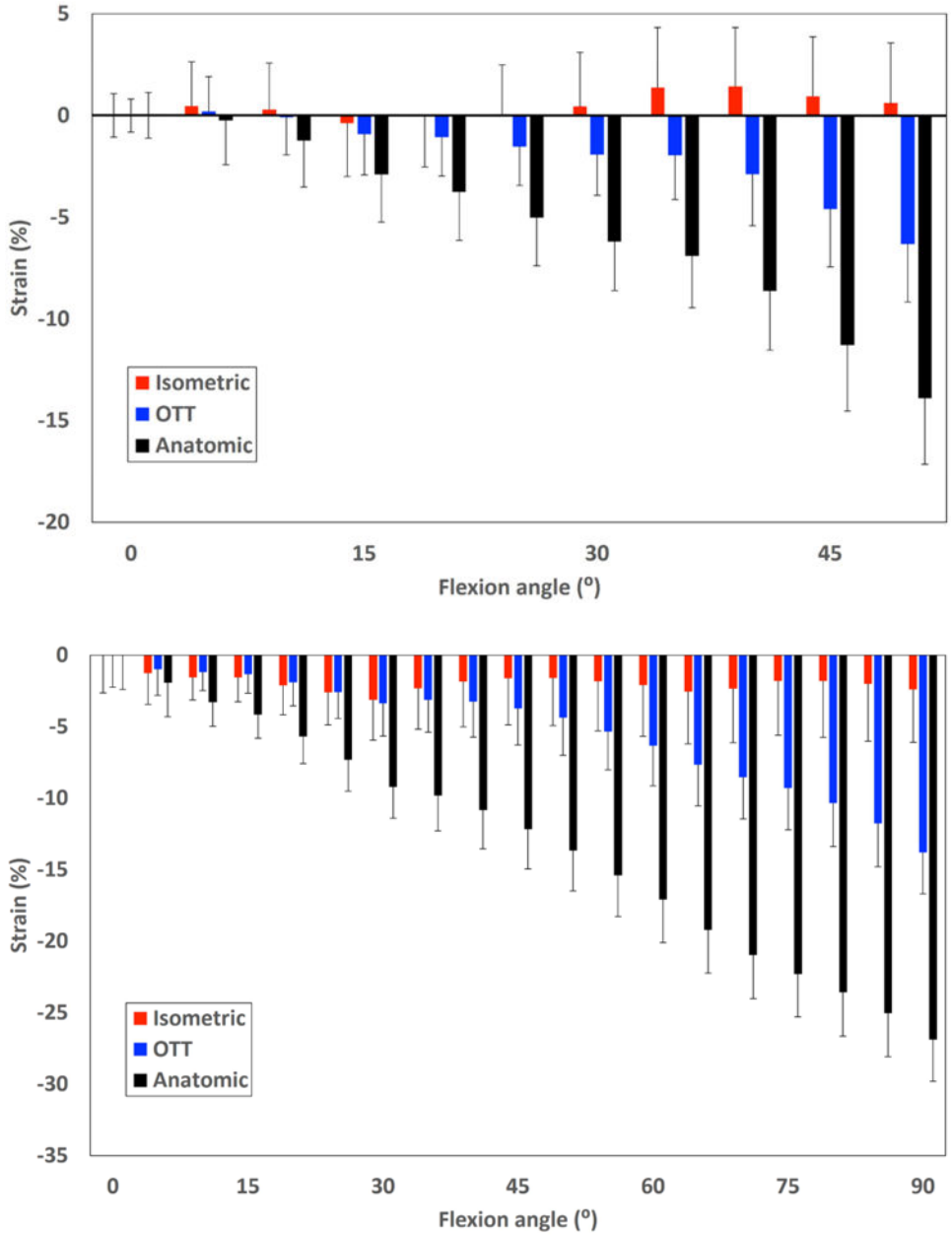

Figure 7.

Strain curves by knee flexion angle for the (**A**) step-up motion and (**B**) sit-to-stand motion, for anatomic, over the top (OTT) and isometric socket positions when connected to the central tibial attachment, where excursion represents strain of the graft relative to 0° of flexion (zero point). Graft strain decreases with increasing flexion angles for the anatomic and OTT socket location whereas the isometric position stays nearly the same.

Table 1

Most isometric graft locations.

	Step-up		Sit-to-stand	
	Length change (% and CI 95)	**Location ($t^{\dagger} \times h^{\ddagger}$)**	**Length change (% and CI 95)**	**Location ($t^{\dagger} \times h^{\ddagger}$)**
Anteromedial	1.7 (1.4 to 1.9)	50 × 14	2.2 (1.9 to 2.5)	43 × 8
Central	1.8 (1.5 to 2.1)	48 × 8	3.1 (2.7 to 3.5)	43 × 8
Posterolateral	2.2 (1.8 to 2.5)	48 × 8	5.2 (4.6 to 5.9)	43 × 8

†*h:* percentage along line *h* (this is perpendicular to the Blumensaat line)

‡*t:* percentage along line *t* (this is parallel to the Blumensaat line)

Table 2

Statistical analysis for isometry of the various studied bundles in the step-up motion (**A**) and sit-to-stand motions (**B**). The three femoral attachments: anatomic ACL center (anatomic), over the top (OTT) and most isometric location; and three tibial locations: anteromedial, central and posterolateral.

(A) Step-up			
Femur Tibia	Anato mic vs Isometric	Anatomic vs OTT	OTT vs Isometric
Anteromedial	$p < 0.001$	$p = 0.01$	$p < 0.001$
Central	$p < 0.001$	$p < 0.001$	$p < 0.001$
Posterolateral	$p < 0.001$	$p < 0.001$	$p < 0.001$
Tibia Femur	Anteromedial vs Central	Anteromedial vs Posterolateral	Central vs Posterolateral
Anatomic	$p = 0.08$	$p < 0.001$	$p = 0.017$
OTT	$p = 0.003$	$p < 0.001$	$p < 0.001$
Isometric	p=0.14	$p < 0.001$	$p = 0.15$
(B) Sit-to-stand			
Femur Tibia	Anatomic vs Isometric	Anatomic vs OTT	OTT vs Isometric
Anteromedial	$p < 0.001$	$p < 0.001$	$p < 0.001$
Central	$p < 0.001$	$p < 0.001$	$p < 0.001$
Posterolateral	$p < 0.001$	$p < 0.001$	$p < 0.001$
Tibia Femur	Anteromedial vs Posterolateral	Anteromedial vs Posterolateral	Central vs Posterolateral
Anatomic	$p = 0.004$	$p < 0.001$	$p < 0.001$
OTT	$p < 0.001$	$p < 0.001$	$p < 0.001$
Isometric	$p = 0.06$	$p < 0.001$	$p = 0.004$

Note: p-values represent statistical significant differences in anisometry (*mean maximum strain – mean minimum strain*).

Table 3

Statistical analysis (results of Tukey's HSD analyses) of between-group length change by knee flexion angle in step-up (**A**) and sit-to-stand (**B**) motion; comparing the anatomic ACL center (anatomic), over the top (OTT), and most isometric bundles when connected to the central tibial location.

(A) Step-up				**(B) Sit-to-stand**			
Flexion angle (°)	**Anatomic vs Isometric**	**Anatomic vs OTT**	**Isometric vs OTT**	**Flexion angle (°)**	**Anatomic vs Isometric**	**Anatomic vs OTT**	**Isometric vs OTT**
0	p = 0.99	p = 0.66	p = 0.63	0	p = 0.99	p = 0.83	p = 0.8
5	p = 0.93	p = 0.93	p = 0.76	5	p = 0.91	p = 0.9	p = 0.68
10	p = 0.33	p = 0.92	p = 0.57	10	p = 0.42	p = 0.94	p = 0.62
15	p = 0.07	p = 0.39	p = 0.65	15	p = 0.04	p = 0.2	p = 0.72
20	p = 0.01	p = 0.06	p = 0.35	20	p < 0.001	p = 0.075	p = 0.26
25	p = 0.010	p = 0.03	p = 0.14	25	p < 0.001	p = 0.009	p = 0.16
30	p < 0.001	p < 0.001	p = 0.03	30	p < 0.001	p = 0.002	p = 0.12
35	p < 0.001	p < 0.001	p = 0.007	35	p < 0.001	p < 0.001	p = 0.03
40	p < 0.001	p < 0.001	p < 0.001	40	p < 0.001	p < 0.001	p = 0.01
45	p < 0.001	p < 0.001	p < 0.001	45	p < 0.001	p < 0.001	p = 0.001
50	p < 0.001	p < 0.001	p < 0.001	50	p < 0.001	p < 0.001	p < 0.001
				55	p < 0.001	p < 0.001	p < 0.001
				60	p < 0.001	p < 0.001	p < 0.001
				65	p < 0.001	p < 0.001	p < 0.001
				70	p < 0.001	p < 0.001	p < 0.001
				75	p < 0.001	p < 0.001	p < 0.001
				80	p < 0.001	p < 0.001	p < 0.001
				85	p < 0.001	p < 0.001	p < 0.001
				90	p < 0.001	p < 0.001	p < 0.001

Note: p-values represent statistical significant differences in strain change between the anatomic, OTT and most isometric bundles.